

This is the accepted manuscript made available via CHORUS. The article has been published as:

## Gain without population inversion in a yoked superfluorescence scheme

Luqi Yuan and Anatoly A. Svidzinsky

Phys. Rev. A **85**, 033836 — Published 29 March 2012

DOI: [10.1103/PhysRevA.85.033836](https://doi.org/10.1103/PhysRevA.85.033836)

# Gain without population inversion in Yoked superfluorescence scheme

Luqi Yuan and Anatoly A. Svidzinsky

*Texas A&M University, College Station TX 77843 and Princeton University, Princeton NJ 08544*

(Dated: March 14, 2012)

We consider a medium composed of three-level (cascade scheme) atoms prepared with coherence between the upper and the ground state (Yoked superfluorescence system). We obtain analytical solution for seed pulses propagation which are resonant with the upper and lower transitions for arbitrary level populations and pulse shapes. We find that if the initial coherence is large enough and intermediate level is populated the system can have gain without population inversion. Coherence can also yield gain suppression in the inverted medium. We obtain conditions for the gain in terms of level populations and coherence.

PACS numbers:

## I. INTRODUCTION

Superradiance (speed up of spontaneous emission) of atomic ensembles is a collective phenomenon which still offers interesting directions of exploration [1]. It was first predicted by Dicke in 1954 [2]. Later on it was observed by Feld and co-workers in HF gas [3] who also gave a theoretical explanation of how an initially inverted two-level system evolves into a superradiant state [4, 5]. Influence of virtual transitions on collective emission and non-local (retardation) effects are among intriguing subjects of current theoretical [6–10] and experimental [11] investigation. Cooperative effects of spontaneous emission can be used for optical quantum-state storage, quantum cryptography [12] and quantum information [13].

Superfluorescence is another collective process in which the superradiant state is developed in a system of initially uncorrelated excited atoms [14]. This process starts with normal spontaneous emission but later develops correlations between the atoms [15]. In the past half century, both types of phenomena, superradiance and superfluorescence, were extensively studied theoretically and experimentally.

Presence of quantum coherence yields interesting effects. In particular, it can lead to superfluorescence without inversion [16–20]. In such systems coherence created by a driving field on one transition influences superfluorescence on another transition. Quantum coherence can also yield lasing without inversion [21–23] which has been extensively studied during the last two decades [24–27].

Yoked superfluorescence [28] is another example of manifestation of quantum coherence. It occurs in a three-level cascade system initially prepared with coherence between the upper and the ground states. Such coherence can be produced by a laser pump pulse propagating through the medium (the direction along the pump we call “forward”, and against the pump “backward”). The laser pulse can excite the upper level from the ground state, e.g., by a two-photon process which creates some initial population in the upper level. Since the intermediate level is initially empty there is population inversion between the upper and the intermediate levels which triggers superfluorescence in this transition. Both experimental and theoretical studies show suppression of the gain in the forward direction [29–31] at early times, when there is no population in the intermediate level, *i.e.* there is population inversion between the upper two levels but no population inversion between the lower two. As soon as the intermediate level becomes populated it decays into the ground state emitting photons mainly in the forward direction [28, 32, 33].

Recently, the generation of backward lasing in air has been demonstrated in the Princeton experiment [34]. In this experiment, the oxygen molecule  $O_2$  is dissociated into two atoms by a strong 226 nm picosecond laser pulse focused into 1 cm long segment. The pulse also excites the oxygen atom from the ground  $2p\ ^3P$  state to the upper  $3p\ ^3P$  state by two-photon absorption which prepares 1 cm long gain medium. The backward 845 nm lasing action was observed between the upper state and the intermediate  $3s\ ^3S$  state. Subsequently a Texas A&M experiment showed that when a strong nanosecond (instead of picosecond) laser pulse is used emission becomes spiky which can be due to effects of coherence [35]. In the Texas A&M experiment the pulse duration ( $\sim 10$  ns) is much longer than the characteristic superfluorescence time scale for the upper transition ( $\sim 100$  ps) and, thus, the intermediate  $3s\ ^3S$  level is being populated.

Having in mind the air laser experiment, we here consider a medium composed of three-level atoms (cascade scheme) which is prepared with arbitrary uniform population distribution. There is also initial coherence between the upper and the ground state levels which is assumed to be generated by a strong multi-photon resonant driving field propagating in the positive (forward)  $z$ -direction. Such generated coherence contains the phase factors  $e^{ikz}$ , where  $k = \omega/c$  and  $\omega$  is the transition frequency. We are interested in propagation of weak seed pulses through the system in forward and backward directions. The pulses have carrier frequency which corresponds to the energy of the upper and lower transitions. We treat the problem semiclassically and use the Maxwell-Bloch equations. In the linear approximation we obtain exact analytical solution for the evolution of an arbitrary initial pulse propagating through the medium. The seed pulse (vacuum fluctuations) undergoes grows or decay depending on the level populations and initial coherence.

We show that for an inverted medium the presence of initial coherence can result in forward gain suppression. This result is known in the literature [29–31]. In addition, we find that coherence can yield gain in the forward direction even if there is no population inversion on both transitions. We obtain conditions for the gain in a general form in terms of level populations and coherences.

## II. EVOLUTION OF WEAK PULSES IN YOKED SUPERFLUORESCENCE SCHEME

Here we consider a medium composed of three-level atoms. Each atom is described by a cascade scheme shown in Fig. 1. The system is uniformly excited by a pump pulse multi-photon resonant with the  $a \leftrightarrow c$  forbidden transition propagating along the  $z$ -axis (forward direction). This process generates coherence  $\rho_{ac}$  between the upper and ground states, thus, there is correlation between atoms. Population can decay through the allowed transitions  $a \rightarrow b$  and  $b \rightarrow c$ . We study how weak seed pulses  $\Omega_{ab}$  and  $\Omega_{bc}$ , having carrier frequency corresponding to the  $a \leftrightarrow b$  and  $b \leftrightarrow c$  transitions, propagate through the medium. In our analytical calculations we assume that during the seed pulse propagation the level populations  $\rho_{aa}$ ,  $\rho_{bb}$  and  $\rho_{cc}$ , as well as coherence  $\rho_{ac}$ , remain constant. However initial seed pulse shapes  $\Omega_{ab}(0, z)$  and  $\Omega_{bc}(0, z)$  are arbitrary.

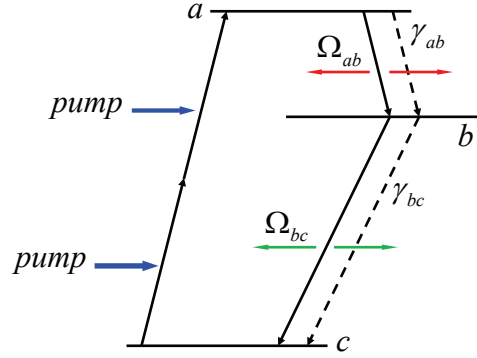


FIG. 1: (Color online) Cascade scheme of atomic energy levels.

We treat the problem semiclassically in the framework of the Maxwell-Bloch equations assuming that electric field and atomic density matrix depend only on coordinate  $z$  and time  $t$ . Equations of motion for the atomic density matrix read

$$\dot{\rho}_{ab}(t, z) = -\Gamma_{ab}\rho_{ab}(t, z) - i\Omega_{ab}(t, z)n_{ab} - i\Omega_{bc}^*(t, z)\rho_{ac}, \quad (1)$$

$$\dot{\rho}_{bc}(t, z) = -\Gamma_{bc}\rho_{bc}(t, z) - i\Omega_{bc}(t, z)n_{bc} + i\Omega_{ab}^*(t, z)\rho_{ac}, \quad (2)$$

where  $n_{ab} = \rho_{aa} - \rho_{bb}$ ,  $n_{bc} = \rho_{bb} - \rho_{cc}$  and  $\rho_{ac}$  are constants,  $\Gamma_{ij} = \Gamma + \gamma_{ij}/2$ ,  $\Gamma$  is the dephasing rate due to collisional broadening and  $\gamma_{ij}$  is the spontaneous decay rate of the corresponding transition. In a more realistic system there is also Doppler broadening and dephasing due to time of atom fly across the active medium. However, in experiments the atomic density is usually greater than  $10^{14} \text{ cm}^{-3}$  and, thus, superradiant time scale is shorter than 10 ps. Hence, line broadening due to superradiant emission is much larger than Doppler broadening ( $\sim 10^{10} \text{ s}^{-1}$ ) and dephasing rate due to time of fly ( $\sim 10^8 \text{ s}^{-1}$ ).

Propagation equations for the electric field are

$$\frac{\partial \Omega_{ab}(t, z)}{\partial z} + \frac{1}{c} \frac{\partial \Omega_{ab}(t, z)}{\partial t} = i\eta_{ab}\rho_{ab}(t, z), \quad (3)$$

$$\frac{\partial \Omega_{bc}(t, z)}{\partial z} + \frac{1}{c} \frac{\partial \Omega_{bc}(t, z)}{\partial t} = i\eta_{bc}\rho_{bc}(t, z), \quad (4)$$

where  $\Omega_{ij}$  is the Rabi frequency corresponding to the electric field envelope,  $\eta_{ij} = 3N\lambda_{ij}^2\gamma_{ij}/8\pi$  is the atom-field interaction constant,  $N$  is the atomic density and  $\lambda_{ij}$  is the transition wavelength. Eqs. (1) and (2) are written for the fields  $\Omega_{ab}$  and  $\Omega_{bc}$  propagating in the forward direction. For the backward propagating fields there is no  $\rho_{ac}$  term in Eqs. (1) and (2) because in this case the phases of  $\rho_{ab}$  and  $\rho_{bc}$  can not match the phase of the coherence  $\rho_{ac}$ . Indeed, for the backward propagation,  $\rho_{ab}$  and  $\rho_{bc}$  have the same phases as the backward fields  $\Omega_{ab}$  and  $\Omega_{bc}$ , that is  $ik_{ab}z$  and  $ik_{bc}z$ . However, the phase of the initial coherence  $\rho_{ac}$  is produced by the forward pump field and has the value  $-i(k_{ab} + k_{bc})z$ . Therefore, for backward direction, the last term in

Eq. (1) has the phase  $-i(k_{ab} + k_{bc})z - ik_{bc}z$ , which differs from the phase of  $\rho_{ab}$  by  $-2i(k_{ab} + k_{bc})z$ . The phase difference leads to a fast oscillating term as a function of  $z$ . In the rotating wave approximation such terms have to be omitted. As a result, solution for the backward propagation can be obtained from the forward one by taking  $\rho_{ac} = 0$ .

We solve Eqs. (1)-(4) with the initial condition  $\rho_{ab}(0, z) = \rho_{bc}(0, z) = 0$  and initial pulse shapes  $\Omega_{ab}(0, z)$  and  $\Omega_{bc}(0, z)$ . Eq. (1) gives

$$\rho_{ab}(t, z) = -in_{ab} \int_0^t \Omega_{ab}(t', z) e^{-\Gamma_{ab}(t-t')} dt' - i\rho_{ac} \int_0^t \Omega_{bc}^*(t', z) e^{-\Gamma_{ab}(t-t')} dt'. \quad (5)$$

Then using Eq. (3) we obtain

$$\frac{\partial \Omega_{ab}(t, z)}{\partial z} + \frac{1}{c} \frac{\partial \Omega_{ab}(t, z)}{\partial t} = \eta_{ab} n_{ab} \int_0^t \Omega_{ab}(t', z) e^{-\Gamma_{ab}(t-t')} dt' + \eta_{ab} \rho_{ac} \int_0^t \Omega_{bc}^*(t', z) e^{-\Gamma_{ab}(t-t')} dt'. \quad (6)$$

Introducing the Laplace transform in time

$$\hat{\Omega}(s, z) = \mathcal{L} \{ \Omega(t, z) \} = \int_0^\infty e^{-st} \Omega(t, z) dt \quad (7)$$

yields

$$\frac{\partial \hat{\Omega}_{ab}(s, z)}{\partial z} + \frac{s}{c} \hat{\Omega}_{ab}(s, z) - \frac{1}{c} \Omega_{ab}(0, z) = \eta_{ab} n_{ab} \frac{\hat{\Omega}_{ab}(s, z)}{s + \Gamma_{ab}} + \eta_{ab} \rho_{ac} \frac{\hat{\Omega}_{bc}^*(s, z)}{s + \Gamma_{ab}}. \quad (8)$$

Similarly for  $\Omega_{bc}$  we obtain the equation

$$\frac{\partial \hat{\Omega}_{bc}^*(s, z)}{\partial z} + \frac{s}{c} \hat{\Omega}_{bc}^*(s, z) - \frac{1}{c} \Omega_{bc}^*(0, z) = \eta_{bc} n_{bc} \frac{\hat{\Omega}_{bc}^*(s, z)}{s + \Gamma_{bc}} - \eta_{bc} \rho_{ac}^* \frac{\hat{\Omega}_{ab}(s, z)}{s + \Gamma_{bc}}. \quad (9)$$

Solution of Eqs. (8) and (9) can be rewritten as

$$\hat{\Omega}_{ab}(s, z) = \frac{1}{c} \int_{-\infty}^z dz' \frac{F(z')}{\lambda_1 - \lambda_2} \left[ e^{\lambda_1(z-z')} - e^{\lambda_2(z-z')} \right], \quad (10)$$

where the source function is

$$F(z) = \frac{\eta_{ab} \rho_{ac}}{s + \Gamma_{ab}} \Omega_{bc}^*(0, z) + \left( \frac{s}{c} - \frac{\eta_{bc} n_{bc}}{s + \Gamma_{bc}} \right) \Omega_{ab}(0, z) + \frac{\partial \Omega_{ab}(0, z)}{\partial z} \quad (11)$$

and the constants  $\lambda_{1,2}$  are

$$\lambda_{1,2} = \frac{1}{2} \left[ \left( -\frac{2s}{c} + \frac{\eta_{ab} n_{ab}}{s + \Gamma_{ab}} + \frac{\eta_{bc} n_{bc}}{s + \Gamma_{bc}} \right) \pm \sqrt{\left( \frac{\eta_{ab} n_{ab}}{s + \Gamma_{ab}} - \frac{\eta_{bc} n_{bc}}{s + \Gamma_{bc}} \right)^2 - 4 \frac{\eta_{ab} \rho_{ac}}{s + \Gamma_{ab}} \frac{\eta_{bc} \rho_{ac}^*}{s + \Gamma_{bc}}} \right]. \quad (12)$$

In the limit that collisional dephasing  $\Gamma$  is much larger than the spontaneous decay rates  $\gamma_{ij}$  we have  $\Gamma_{ab} \approx \Gamma_{bc} \approx \Gamma$  and constants  $\lambda_{1,2}$  reduce to

$$\lambda_{1,2} = -\frac{s}{c} - \frac{\xi_{1,2}}{s + \Gamma}, \quad (13)$$

where

$$\xi_{1,2} = -\frac{1}{2} [\eta_{ab} n_{ab} + \eta_{bc} n_{bc} \pm \zeta], \quad (14)$$

$$\zeta = \sqrt{(\eta_{ab} n_{ab} - \eta_{bc} n_{bc})^2 - 4 \eta_{ab} \eta_{bc} |\rho_{ac}|^2}. \quad (15)$$

In this limit the inverse Laplace transform of Eq. (10) yields the following final answer for pulse evolution in the forward direction

$$\Omega_{ab}(t, z) = \Omega_{ab}(0, z - ct) + \int_{z-ct}^z dz' \Omega_{ab}(0, z') e^{-\frac{\Gamma}{c}(z' + ct - z)}$$

$$\begin{aligned}
& \times \left\{ \frac{\xi_1 + \eta_{bc} n_{bc}}{\zeta} \sqrt{\frac{\xi_1(z-z')/c}{z'+ct-z}} J_1 \left[ 2\sqrt{\frac{\xi_1}{c}}(z-z')(z'+ct-z) \right] \right. \\
& \left. - \frac{\xi_2 + \eta_{bc} n_{bc}}{\zeta} \sqrt{\frac{\xi_2(z-z')/c}{z'+ct-z}} J_1 \left[ 2\sqrt{\frac{\xi_2}{c}}(z-z')(z'+ct-z) \right] \right\} \\
& - \int_{z-ct}^z dz' \frac{\eta_{ab} \rho_{ac}}{\zeta} \Omega_{bc}^*(0, z') e^{-\frac{\Gamma}{c}(z'+ct-z)} \left\{ \sqrt{\frac{\xi_1(z-z')/c}{z'+ct-z}} J_1 \left[ 2\sqrt{\frac{\xi_1}{c}}(z-z')(z'+ct-z) \right] \right. \\
& \left. - \sqrt{\frac{\xi_2(z-z')/c}{z'+ct-z}} J_1 \left[ 2\sqrt{\frac{\xi_2}{c}}(z-z')(z'+ct-z) \right] \right\}, \tag{16}
\end{aligned}$$

where  $\xi_{1,2}$  and  $\zeta$  are defined in Eqs. (14) and (15),  $J_1(z)$  is the Bessel function. Similarly, the solution for the field  $\Omega_{bc}$  reads

$$\begin{aligned}
\Omega_{bc}^*(t, z) &= \Omega_{bc}^*(0, z-ct) + \int_{z-ct}^z dz' \Omega_{bc}^*(0, z') e^{-\frac{\Gamma}{c}(z'+ct-z)} \\
& \times \left\{ \frac{\xi_1 + \eta_{ab} n_{ab}}{\zeta} \sqrt{\frac{\xi_1(z-z')/c}{z'+ct-z}} J_1 \left[ 2\sqrt{\frac{\xi_1}{c}}(z-z')(z'+ct-z) \right] \right. \\
& \left. - \frac{\xi_2 + \eta_{ab} n_{ab}}{\zeta} \sqrt{\frac{\xi_2(z-z')/c}{z'+ct-z}} J_1 \left[ 2\sqrt{\frac{\xi_2}{c}}(z-z')(z'+ct-z) \right] \right\} \\
& + \int_{z-ct}^z dz' \frac{\eta_{bc} \rho_{ac}^*}{\zeta} \Omega_{ab}(0, z') e^{-\frac{\Gamma}{c}(z'+ct-z)} \left\{ \sqrt{\frac{\xi_1(z-z')/c}{z'+ct-z}} J_1 \left[ 2\sqrt{\frac{\xi_1}{c}}(z-z')(z'+ct-z) \right] \right. \\
& \left. - \sqrt{\frac{\xi_2(z-z')/c}{z'+ct-z}} J_1 \left[ 2\sqrt{\frac{\xi_2}{c}}(z-z')(z'+ct-z) \right] \right\}. \tag{17}
\end{aligned}$$

To obtain the evolution of the backward pulse we put  $\rho_{ac} = 0$  in the above equations and find

$$\begin{aligned}
\Omega_{ab}(t, z) &= \Omega_{ab}(0, z-ct) + \\
& \sqrt{\frac{\eta_{ab} n_{ab}}{c}} \int_{z-ct}^z dz' \Omega_{ab}(0, z') e^{-\frac{\Gamma}{c}(z'+ct-z)} \sqrt{\frac{z-z'}{z'+ct-z}} I_1 \left[ 2\sqrt{\frac{\eta_{ab} n_{ab}}{c}} \sqrt{(z-z')(z'+ct-z)} \right], \tag{18}
\end{aligned}$$

$$\begin{aligned}
\Omega_{bc}(t, z) &= \Omega_{bc}(0, z-ct) + \\
& \sqrt{\frac{\eta_{bc} n_{bc}}{c}} \int_{z-ct}^z dz' \Omega_{bc}(0, z') e^{-\frac{\Gamma}{c}(z'+ct-z)} \sqrt{\frac{z-z'}{z'+ct-z}} I_1 \left[ 2\sqrt{\frac{\eta_{bc} n_{bc}}{c}} \sqrt{(z-z')(z'+ct-z)} \right], \tag{19}
\end{aligned}$$

where  $I_1(z)$  is the modified Bessel function.

Eqs. (16)-(19) give the exact analytical answer on how initial weak pulses  $\Omega_{ab}(0, z)$  and  $\Omega_{bc}(0, z)$  propagate through the medium. As an illustration, we consider a simple example of  $\delta$ -function initial pulse  $\Omega_{ab}(0, z) = \Omega_{ab}^{(0)} \delta(z)$  and no initial pulse at the  $b \leftrightarrow c$  transition  $\Omega_{bc}(0, z) = 0$ . Then Eqs. (16) and (17) yield for forward direction

$$\Omega_{ab}(t, z) = \Omega_{ab}^{(0)} \delta(z-ct) + \Omega_{ab}^{(0)} e^{-\Gamma(t-z/c)} \left\{ \frac{\xi_1 + \eta_{bc} n_{bc}}{\zeta} \sqrt{\frac{\xi_1 z/c}{ct-z}} J_1 \left[ 2\sqrt{\frac{\xi_1}{c}} z(ct-z) \right] \right.$$

$$- \frac{\xi_2 + \eta_{bc} n_{bc}}{\zeta} \sqrt{\frac{\xi_2 - z/c}{ct - z}} J_1 \left[ 2 \sqrt{\frac{\xi_2}{c}} z (ct - z) \right] \Big\} \theta(ct - z), \quad (20)$$

$$\Omega_{bc}^*(t, z) = \frac{\eta_{bc} \rho_{ac}^*}{\zeta} \Omega_{ab}^{(0)} e^{-\Gamma(t-z/c)} \times \left\{ \sqrt{\frac{\xi_1 z/c}{ct - z}} J_1 \left[ 2 \sqrt{\frac{\xi_1}{c}} z (ct - z) \right] - \sqrt{\frac{\xi_2 z/c}{ct - z}} J_1 \left[ 2 \sqrt{\frac{\xi_2}{c}} z (ct - z) \right] \right\} \theta(ct - z). \quad (21)$$

For the backward direction we obtain

$$\Omega_{ab}(t, z) = \Omega_{ab}^{(0)} \delta(z - ct) + \sqrt{\frac{\eta_{ab} n_{ab}}{c}} \Omega_{ab}^{(0)} e^{-\frac{\Gamma}{c}(ct-z)} \sqrt{\frac{z}{ct - z}} I_1 \left[ 2 \sqrt{\frac{\eta_{ab} n_{ab}}{c}} \sqrt{z(ct - z)} \right] \theta(ct - z), \quad (22)$$

$$\Omega_{bc}(t, z) = 0. \quad (23)$$

The first term in Eqs. (20) and (22) corresponds to the initial seed pulse propagating in free space. The other terms are coming from the interaction between atoms and electric field.

### III. FORWARD GAIN SUPPRESSION AND FORWARD GAIN WITHOUT POPULATION INVERSION

We assume that atomic sample is  $L = 1$  cm long, so it takes 0.033 ns for the photon to travel through the system. Density of atoms is large enough so that the coupling constants are  $\eta = \eta_{ab} = \eta_{bc} = 1000 \text{ cm}^{-1} \text{ ns}^{-1}$ . We take the dephasing rate  $\Gamma = 1 \text{ ns}^{-1}$ . Pulse evolution is mainly governed by collective (superradiant) effects and occurs on a time scale much faster than the dephasing time. Thus assumption about constant  $\rho_{ac}$  is valid.

In Fig. 2 we plot the output fields  $\Omega_{ab}(t, z)$  and  $\Omega_{bc}(t, z)$  given by Eqs. (20)-(22) at the edge of the sample  $z = L$  as a function of time. We assume the following population distribution  $\rho_{aa} = 0.2$ ,  $\rho_{bb} = 0.05$ ,  $\rho_{cc} = 0.75$  and coherence  $\rho_{ac} = \sqrt{0.15}i$ . Both forward and backward fields at the  $a \rightarrow b$  transition are shown. Please note that in the plot we do not show the  $\delta$ -function term in Eqs. (20) and (22).

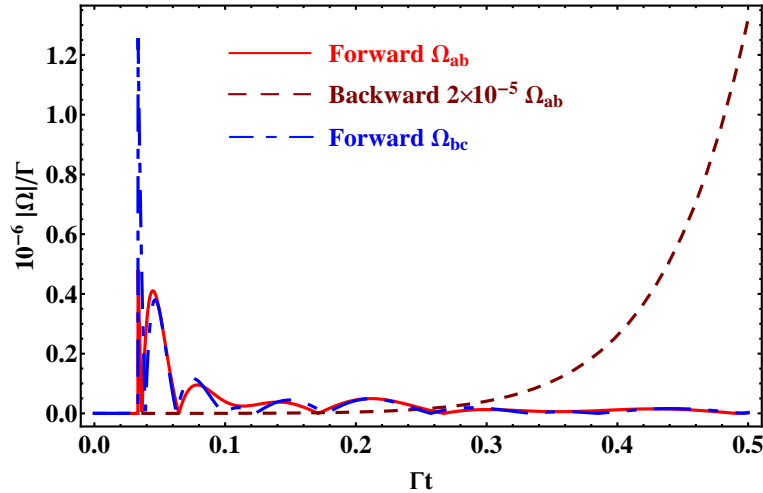


FIG. 2: (Color online) Output fields at the edge of the sample as a function of time given by Eqs. (20)-(22) with population distribution  $\rho_{aa} = 0.2$ ,  $\rho_{bb} = 0.05$ ,  $\rho_{cc} = 0.75$  and coherence  $\rho_{ac} = \sqrt{0.15}i$ . Solid line shows output forward field at the  $a \rightarrow b$  transition, dashed line is the output backward field at the  $a \rightarrow b$  transition divided by  $5 \times 10^4$ , while dash-dot line is the forward field at the  $b \rightarrow c$  transition.

Emission in the backward direction grows exponentially with time as expected for the inverted medium (in the present example there is population inversion between levels  $a$  and  $b$ ). According to Eq. (22) it follows asymptotic of the modified Bessel function. However, forward emission is affected by the coherence  $\rho_{ac}$ . The presence of such coherence makes the forward field oscillate

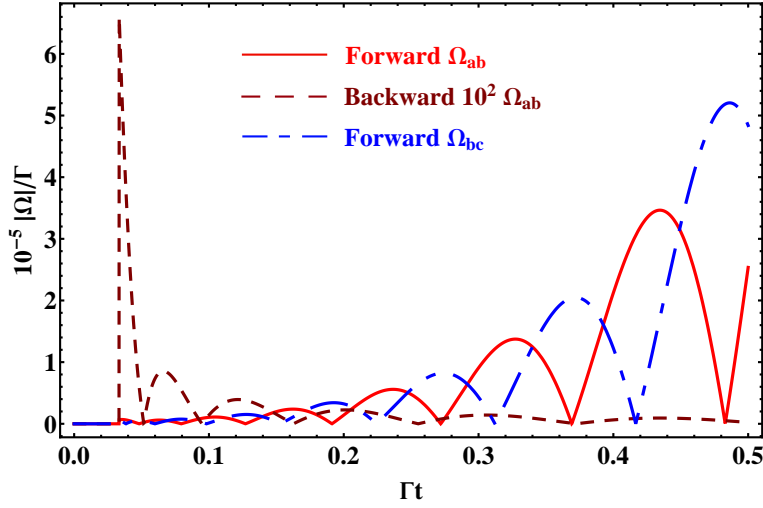


FIG. 3: (Color online) Output fields at the edge of the sample as a function of time given by Eqs. (20)-(22) with population distribution  $\rho_{aa} = 0.1$ ,  $\rho_{bb} = 0.3$ ,  $\rho_{cc} = 0.6$  and coherence  $\rho_{ac} = \sqrt{0.06}i$ . Solid line shows output forward field at the  $a \rightarrow b$  transition, dashed line is the output backward field at the  $a \rightarrow b$  transition multiplied by 100, while dash-dot line is the forward field at the  $b \rightarrow c$  transition.

and decay at large time. This behavior indicates a forward gain suppression which was previously reported in the literature [28, 29]. The forward field on the  $b \rightarrow c$  transition shows similar features. In the present example we do not include the backward field on the  $b \rightarrow c$  transition [36].

Next we take the population distribution  $\rho_{aa} = 0.1$ ,  $\rho_{bb} = 0.3$ ,  $\rho_{cc} = 0.6$  and coherence  $\rho_{ac} = \sqrt{0.06}i$ . Now there is no population inversion in both transitions. The output fields  $\Omega_{ab}(t, z)$  and  $\Omega_{bc}(t, z)$  at the edge of the sample are shown in Fig. 3. In the present example the backward field in the  $a \rightarrow b$  transition decays because there is no population inversion. Namely, for  $n_{ab} < 0$  Eq. (22) yields

$$\Omega_{ab}(t, z) = \Omega_{ab}^{(0)} \delta(z - ct) - \sqrt{\frac{\eta_{ab}|n_{ab}|}{c}} \Omega_{ab}^{(0)} e^{-\frac{\Gamma}{c}(ct-z)} \sqrt{\frac{z}{ct-z}} J_1 \left[ 2\sqrt{\frac{\eta_{ab}|n_{ab}|}{c}} \sqrt{z(ct-z)} \right] \theta(ct - z), \quad (24)$$

that is pulse decays according to the asymptotic of the Bessel function  $J_1$ . However, coherence  $\rho_{ac}$  yields enhancement of both forward fields  $\Omega_{ab}(t, z)$  and  $\Omega_{bc}(t, z)$ . Thus, there is forward gain without population inversion in our system.

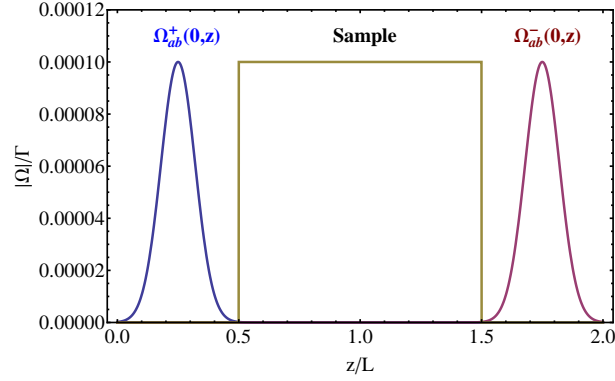


FIG. 4: (Color online) Gaussian-shape initial seed pulses for the forward and backward fields used in numerical simulations

In addition to our analytical results we solve the full Maxwell-Bloch equations numerically including population dynamics and pulse propagation both in forward and backward directions. In numerical simulations, instead of delta function, Gaussian-shape pulses are used for the initial seed for forward and backward fields at the  $a \rightarrow b$  transition (see Fig. 4). The FWHM of the seed pulse is taken as  $\Delta z = 0.167L$ . The results of simulations are shown in Fig. 5. Numerical solution exhibits similar features as the analytical result with delta function seed. When there is population inversion between levels  $a$  and  $b$ , the numerical simulations show the forward gain suppression in the  $a \rightarrow b$  transition (see Fig. 5a), while with no population inversion there is forward gain (see Fig. 5b).

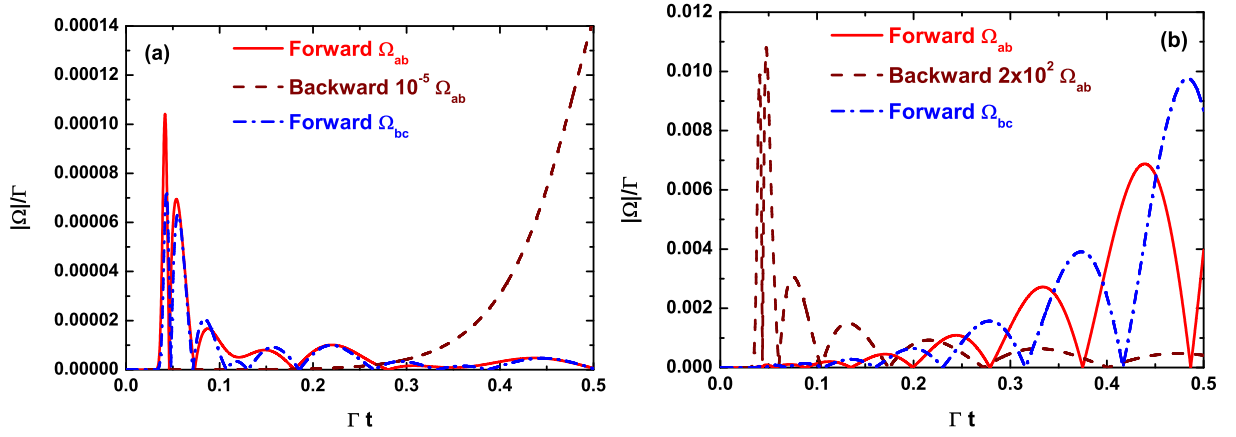


FIG. 5: (Color online) Output fields at the edge of the sample as a function of time obtained by numerical solution of the Maxwell-Bloch equations with Gaussian seed pulses and initial conditions  $\rho_{aa} = 0.2$ ,  $\rho_{bb} = 0.05$ ,  $\rho_{cc} = 0.75$ ,  $\rho_{ac} = \sqrt{0.15}i$  (a) and  $\rho_{aa} = 0.1$ ,  $\rho_{bb} = 0.3$ ,  $\rho_{cc} = 0.6$ ,  $\rho_{ac} = \sqrt{0.06}i$  (b).

To show that lasing would also occur starting from atomic fluctuations we calculated numerically forward and backward emission using quantum noise as a seed instead of sending seed pulses. We found that if there is gain in the medium then simulations with the seed pulses and noise give very similar results. Thus, our analysis based on the seed pulse propagation adequately describes system's evolution.

#### IV. CONDITIONS FOR GAIN IN FORWARD DIRECTION

Analytical results we obtained allow us to find condition for positive gain in the forward direction. If we disregard dephasing  $\Gamma$  the gain is positive if  $\zeta$  in Eq. (15) is imaginary which yields condition

$$4\eta_{ab}\eta_{bc}|\rho_{ac}|^2 > (\eta_{ab}n_{ab} - \eta_{bc}n_{bc})^2. \quad (25)$$

Also gain is positive if  $\xi_1$  or  $\xi_2$  have negative real part, that is

$$\eta_{ab}n_{ab} + \eta_{bc}n_{bc} + \sqrt{(\eta_{ab}n_{ab} - \eta_{bc}n_{bc})^2 - 4\eta_{ab}\eta_{bc}|\rho_{ac}|^2} > 0. \quad (26)$$

If  $\eta_{ab} = \eta_{bc}$  then conditions (25) and (26) reduce to

$$2|\rho_{ac}| > |n_{ab} - n_{bc}| = |1 - 3\rho_{bb}|, \quad (27)$$

$$\rho_{aa} - \rho_{cc} + \sqrt{(1 - 3\rho_{bb})^2 - 4|\rho_{ac}|^2} > 0. \quad (28)$$

If one of the inequalities (27) and (28) is satisfied then there is positive gain in the forward direction. If  $\rho_{ac} = 0$  then Eq. (28) yields the requirement that  $\rho_{aa} > \rho_{bb}$ . If we increase  $|\rho_{ac}|$  then condition (28) may no longer be satisfied even if there is population inversion between levels  $a$  and  $b$ . This yields forward gain suppression due to coherence. However, if  $|\rho_{ac}|$  is large enough and level  $b$  is populated ( $\rho_{bb} \neq 0$ ) then one can fulfil inequality (27) even if there is no population inversion on the  $a \rightarrow b$  and  $b \rightarrow c$  transitions. In this range of parameters the system has forward gain without inversion. Please note that the requirement  $\rho_{bb} \neq 0$  is crucial and, thus, to observe such a regime one should wait until level  $b$  becomes populated.

Physics behind our results can be understood by noting an analogy between Eqs. (1)-(4) and equations of motion of the coupled damped harmonic oscillators. Let us consider spatially uniform case assuming that medium, as well as pulses, is infinitely long. Then, introducing notations  $\Omega_{ab} = x$  and  $\Omega_{bc} = y$  Eqs. (1)-(4) can be written as

$$\ddot{x} + \Gamma_{ab}\dot{x} - c\eta_{ab}n_{ab}x - c\eta_{ab}\rho_{ac}y = 0, \quad (29)$$

$$\ddot{y} + \Gamma_{bc}\dot{y} - c\eta_{bc}n_{bc}y + c\eta_{bc}\rho_{ac}x = 0. \quad (30)$$



These equations show that coherence  $\rho_{ac}$  provides coupling between the two oscillators. Equilibrium point  $x = y = 0$  is unstable (positive gain) if the oscillator matrix

$$\begin{pmatrix} c\eta_{ab}n_{ab} & c\eta_{ab}\rho_{ac} \\ -c\eta_{bc}\rho_{ac} & c\eta_{bc}n_{bc} \end{pmatrix} \quad (31)$$

has eigenvalues which are complex or have positive real part. Taking into account that matrix eigenvalues are

$$\lambda_{1,2} = \frac{c}{2} \left( \eta_{ab}n_{ab} + \eta_{bc}n_{bc} \pm \sqrt{(\eta_{ab}n_{ab} - \eta_{bc}n_{bc})^2 - 4\eta_{ab}\eta_{bc}|\rho_{ac}|^2} \right) \quad (32)$$

we obtain conditions for the gain which coincide with Eqs. (25) and (26). So, physics behind forward gain without inversion and forward gain suppression with inversion is the same as physics of stability of the coupled harmonic oscillators.

## V. CONCLUSION

In this paper, we consider pulse propagation through a medium composed of three-level (cascade scheme) atoms with initial coherence between the upper and ground states. We obtain analytical solutions for pulse evolution for arbitrary initial populations and pulse shapes. Emission in the forward direction is similar to Yoked superfluorescence, that is there is simultaneous emission on the upper and lower transitions. We find that initial coherence can result in gain in the forward direction without inversion if the intermediate level is populated. On the other hand, coherence can suppress forward gain even in inverted medium.

In the air laser experiment [35] it is likely that the system undergoes both regimes. In this experiment, the pump pulse first excites partially the upper level  $a$  which produces population inversion between the upper two levels. This yields backward lasing at early time, which transfers the population from the upper level to the middle level  $b$ . During this process, the forward gain is suppressed. After some time, the upper state population is depleted. This promotes the system into the state with  $\rho_{aa} < \rho_{bb} < \rho_{cc}$  while the long pump pulse continues to generate coherence  $\rho_{ac}$ . For these conditions the forward gain can be achieved as we show here. These processes are repeated as long as the pump field is on.

Our work combines lasing and superradiance together. In the case of a laser (with or without inversion) a weak seed pulse exponentially grows in the linear regime. In the case of superradiance in extended medium the emitted pulse decays undergoing oscillations with the collective frequency. The present problem combines these two effects which yields a possibility of exponential grow and oscillations of the pulse at the same time.

## Acknowledgments

The authors thank Marlan O. Scully for helpful discussion. We gratefully acknowledge support for this work by National Science Foundation Grant EEC-0540832 (MIRTHE ERC), the Office of Naval Research, and the Robert A. Welch Foundation (A-1261). L. Y. is supported by the Herman F. Heep and Minnie Belle Heep Texas A&M University Endowed Fund held/administered by the Texas A&M Foundation.

- 
- [1] M.O. Scully and A.A. Svidzinsky, *Science* **325**, 1510 (2009).
  - [2] R.H. Dicke, *Phys. Rev.* **93**, 99 (1954).
  - [3] N. Skribanowitz, I.P. Herman, J.C. MacGillivray, and M.S. Feld, *Phys. Rev. Lett.* **30**, 309 (1973).
  - [4] J.C. MacGillivray and M.S. Feld, *Phys. Rev. A* **14**, 1169 (1976).
  - [5] J.C. MacGillivray and M.S. Feld, *Phys. Rev. A* **23**, 1334 (1981).
  - [6] A.A. Svidzinsky, J.T. Chang and M.O. Scully, *Phys. Rev. Lett.* **100**, 160504 (2008).
  - [7] M.O. Scully, *Phys. Rev. Lett.* **102**, 143601 (2009).
  - [8] R. Friedberg and J.T. Manassah, *Phys. Lett. A* **374**, 1648 (2010).
  - [9] A.A. Svidzinsky, J.T. Chang and M.O. Scully, *Phys. Rev. A* **81**, 053821 (2010).
  - [10] A.A. Svidzinsky, *Optics Communications* **284**, 269 (2011); A.A. Svidzinsky, *Phys. Rev. A* **85**, 013821 (2012).
  - [11] R. Röhlsberger, K. Schlage, B. Sahoo, S. Couet and R. Ruffer, *Science* **328**, 1248 (2010).
  - [12] A. Kalachev and S. Kröll, *Phys. Rev. A* **74**, 023814 (2006).
  - [13] D. Porras and J.I. Cirac, *Phys. Rev. A* **78**, 053816 (2008).
  - [14] R. Bonifaci and L.A. Lugiato, *Phys. Rev. A* **11**, 1507 (1975); *Phys. Rev. A* **12**, 587 (1975).
  - [15] S. Prasad and R.J. Glauber, *Phys. Rev. A* **31**, 1583 (1985).
  - [16] V.A. Malyshev, F. Carreño, M.A. Antón, O.G. Calderón, and F. Domínguez-Adame, *J. Opt. B* **5**, 313 (2003).
  - [17] V. Kozlov, O. Kocharovskaya, Y. Rostovtsev, and M. Scully, *Phys. Rev. A* **60** 1598 (1999).

- [18] V.A. Malyshev, I.V. Ryzhov, E.D. Trifonov, and A.I. Zaitsev, *Laser Phys.* **8** 494 (1998).
- [19] A.I. Zaitsev, I.V. Ryzhov, E.D. Trifonov, and V.A. Malyshev, *Laser Phys.* **9** 876 (1999).
- [20] A.A. Bogdanov, A.I. Zaitsev, and I.V. Ryzhov, *Opt. Spectrosc.* **89**, 1012 (2000).
- [21] O.A. Kocharovskaya and Ya. I. Khanin, *Zh. Eksp. Teor. Phys.* **90** 1610 (1986) [*JETP* **63** 945 (1986)]; *Pis'ma Zh. Eksp. Teor. Fiz.* **48**, 581 (1988) [*JETP Lett.* **48**, 630 (1988)].
- [22] S.E. Harris, *Phys. Rev. Lett.* **62**, 1033 (1989).
- [23] M.O. Scully and M.S. Zubairy, *Quantum Optics* (Cambridge University Press, Cambridge, UK, 1997).
- [24] A.S. Manka, J.P. Dowling, C.M. Bowden, and M. Fleischhauer, *Quantum Opt.* **6**, 371 (1994).
- [25] O. Kocharovskaya, *Hyperfine Interact.* **107**, 187 (1997).
- [26] J. Mompart and R. Corbalán, *J. Opt. B* **2**, R7 (2000).
- [27] M.O. Scully and M. Fleischhauer, *Science* **263**, 337 (1994).
- [28] J.H. Brownell, X. Lu, and S.R. Hartmann, *Phys. Rev. Lett.* **75**, 3265 (1995).
- [29] W. R. Garrett, *Phys. Rev. Lett.* **70**, 4059 (1993).
- [30] J.T. Manassah and I. Gladkova, *Opt. Commun.* **179**, 51 (2000).
- [31] H. Brownell, B. Gross, X. Lu, S.R. Hartmann, and J.T. Manassah, *Laser Phys.* **3**, 509 (1993).
- [32] D. Felinto, L.H. Acioli, and S.S. Vianna, *Opt. Lett.* **25**, 917 (2000).
- [33] G.O. Ariunbold, M.M. Kash, V.A. Sautenkov, H. Li, Y.V. Rostovtsev, G.R. Welch, and M.O. Scully, *Phys. Rev. A* **82**, 043421 (2010).
- [34] A. Dogariu, J. B. Michael, M. O. Scully, and R. B. Miles, *Science* **331**, 442 (2011).
- [35] A. J. Traverso *et al.*, *Coherence Brightened Laser Source for Atmospheric Remote Sensing* (preprint).
- [36] The initial seed for the backward field on the  $b \rightarrow c$  transition will only be amplified if there is population inversion between the lower two levels. In the present example, there is no population inversion between  $b$  and  $c$  levels, so we do not include seed field for this transition in our plot.